# AN IMPROVED WORKFLOW FOR IMAGE- AND LASER-BASED VIRTUAL GEOLOGICAL OUTCROP MODELLING

A. Sima [a, *], S. J. Buckley [a], D. Schneider [b], J. A. Howell [a]

[a] Uni CIPR, Postboks 7810, N-5020 Bergen, Norway
(aleksandra.sima, simon.buckley, john.howell)@uni.no
[b] Technische Universität Dresden, Institute of Photogrammetry and Remote Sensing, 01062 Dresden, Germany
danilo.schneider@tu-dresden.de

**Commission III, WG III/2**

KEY WORDS: TLS, Integration, Visualization, Photogrammetry, Geology

**ABSTRACT:**

This paper reports on research that aims to enhance the existing workflow for virtual geological outcrop modelling. Combining laser scanning and photogrammetric data in an automated processing chain makes the virtual models more accessible for non-specialists. An essential part of the proposed workflow is based on automated image feature extraction and registration routines, to minimize the manual time spent on post-processing, and to improve the coherence of the virtual outcrop data. It is anticipated that the final results of the research will provide the geologist with a more reliable means for digital data interpretation.

## 1. INTRODUCTION

### 1.1 Background

Many earth science applications are benefitting from advances made to laser scanning and photogrammetric hardware and processing algorithms. One such area where these techniques have provided great benefit is in the study and 3D modelling of geological outcrops. These outcrops are exposed cliff sections or quarries (Figure 1), which are used as analogues for subsurface hydrocarbon reservoirs, aquifers and sites for potential $CO_2$ sequestration, for helping to improve understanding of geometrical relationships between geological features.

Figure 1. Outcrops of Ferron Sandstone, Ivie Creek, Utah

Traditionally, data were collected with relatively crude spatial accuracy, using sedimentary logging, photomontaging and architectural panels, resulting in more qualitative studies (e.g. Mountney et al., 1998). However, recent developments to digital data collection methods, especially those involving digital photogrammetry and terrestrial or helicopter-based laser scanning techniques, overcome the limitations of spatial accuracy, allowing quantitative aspects to be improved.

The potential of laser scanning combined with image acquisition has been proven and geomatics is becoming prevalent in the field of outcrop geology. Methods for creating high-accuracy and high-resolution 3D photorealistic models of geological outcrops, used to guide the building of geocellular reservoir models and the extraction of statistical data, are now widespread (Bellian et al., 2005; Pringle et al., 2006, Buckley et al., 2008). However, so far the great potential for improved integration of imagery and laser data has not yet been realised. Further research is required to improve and automate key aspects of the workflow before such methods are standardized across geological research and industry.

### 1.2 Motivation

The workflow for collecting and using virtual outcrop data has been developed and successfully applied in reservoir modelling in recent years (Enge et al., 2007; Buckley et al., 2008a; Buckley et al., 2008b). The current project aims to enhance the existing workflow for processing laser scanning and photogrammetric data, so that automation is improved, making the procedure more accessible for non-specialists. An essential part of the modified workflow is based on automated image feature extraction and registration routines, to minimize the manual time spent on post-processing of the virtual outcrop data.

## 2. DATA CHARACTERISTICS

The datasets used in the project were acquired from both ground- and oblique helicopter-based laser scanning.

* Corresponding author.

### 2.1 Terrestrial data

In the case of terrestrial scanning, a Riegl LMS-Z420i scanner is used in a combination with a calibrated Nikon D200 10 megapixel camera. The maximum range of scanner is quoted as 1000m, and it can acquire points with a rate up to 11,000 points per second, with a quoted accuracy of 0.01m (one sigma) at 50m range (Riegl, 2010). In order to ensure sufficient prerequisites for the relative scan registration, the adjacent scans are acquired with overlap greater than 10% of the area (Bellian et al., 2005).

Depending on the characteristics and accessibility of the scanned outcrop section, Nikkor 85 mm, 50 mm or 14 mm lenses are mounted on the Nikon D200 camera (CCD pixel size of 6.1µm). The lenses are periodically calibrated and the focal lengths are fixed for the duration of the data collection. The orientation of the camera is calibrated relative to the scanner centre so that the imagery can be easily registered in the project coordinate system and further used as a texture source in the photorealistic virtual model. In order to ensure optimal texture mapping conditions the photos should be collected so that the image rays are as close to normal to the outcrop face if possible (Debevec et al., 1996). If needed, additional freehand photos can be also acquired. In this case manual selection of tie points between the point cloud and images is needed.

In order to register the acquired dataset into a geodetic coordinate system a single frequency Global Navigation Satellite System (GNSS) antenna is mounted above the camera in a distance calibrated relative to the scanner centre. The scanner position is logged with a rate of 10Hz during the data acquisition period, and further post-processed relative to a nearby base station.

### 2.2 Helicopter-based data collection

The Helimap system used from a helicopter platform consists of a Riegl LMS Q240i-60 airborne laser scanner and a Hasselblad H1 camera. The maximum range of the scanner at 80% reflectance is equal to 450m. Data are collected with a rate computed as a function of desired point density and flight parameters, up to 10,000 points per second, with a quoted accuracy of 0.02m (one sigma) at 50m range (Riegl, 2010).

The Hasselblad H1 camera provides 22 megapixel RGB images (5448x4080) with 9µm pixel size that can be acquired with a calibrated lens with focal length of 35mm (Skaloud et al., 2002).

The camera and the scanner are rigidly coupled and their position is constantly logged by the GNSS/INS positioning system. A combination of a dual frequency GNSS receiver and an iMar iIMU-FSAS tactical grade inertial measurement unit supplies, after the lever arm and the boresight calibration, the information necessary to recreate the point cloud and camera orientation parameters. Oblique and nadir scanning can be performed with the same system configuration and the same accuracy. The mapping accuracy of the DSM/DTM data delivered by the Helimap system was determined as <0.15m (Vallet, 2007).

## 3. PROCESSING WORKFLOW

The currently existing workflow for creation of virtual outcrop models is capable of handling both types of data, terrestrial and helicopter-based. Regardless of the data collection mode used, the principles of the data processing are similar and are presented in Figure 2.

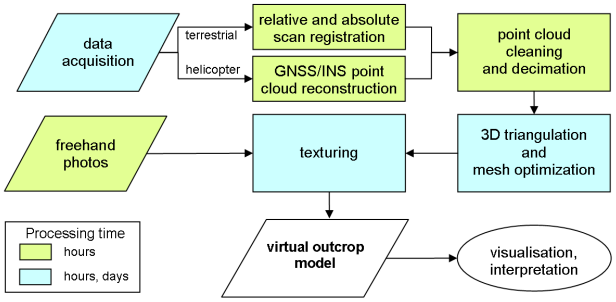


Figure 2. General processing workflow

The size of the dataset resulting from the acquisition depends on the size of the scanned outcrop and the density of the point cloud, but may be millions of 3D points and hundreds of digital images, covering hundreds of meters, or in the case of helicopter-based datasets, tens of kilometres of outcrop. The general data processing workflow is similar for the ground- and helicopter-based datasets. For the sake of simplicity, a processing chain only for the case of data collected from the ground is sketched in this paper. For the helicopter-based workflow, see Buckley et al., 2008b.

### 3.1 Data registration

All the data collected by the terrestrial scanner are managed by Riscan PRO®, the companion software for the Riegl terrestrial scanner series (Riegl, 2010). In the first phase of the data processing all the scans are registered into a single coordinate system. The preliminary rough scan alignment is performed manually by marking several common points between the adjacent scans in the IMAlign module of PolyWorks® (Innovmetric, 2010). Then, a spatial rotation, translation and uniform scaling of each scan with respect to the reference scan (a single scan held fixed in the centre of each cliff section) are derived using the implemented version of the iterative closest point algorithm (e.g. Besl and McKay, 1992). Resulting transformation matrices enable the creation of a single point cloud of all the scans of the cliff section. The project coordinates can easily be transformed to a geodetic coordinate system using the scanner positions derived from the post-processed GNSS observations.

### 3.2 Point cloud cleaning and decimation

In order to make data handling more comfortable, the datasets should be of manageable sizes. This size is rapidly changing and depends on the hardware and software capabilities. Nevertheless, in addition to the overall point cloud decimation, reduction of the point density in overlapping areas is needed. The automatic random, uniform or curvature-based point cloud thinning function of IMEdit module of PolyWorks® is used to reduce the overall number of points and the remaining processing time.

### 3.3 Triangulation and mesh optimization

In order to create a photorealistic (textured) virtual the topographic surface is represented by a Triangulated Irregular Network (TIN). The decimated point cloud is triangulated using a tolerance-based meshing algorithm in the IMEdit module of PolyWorks®. Correct triangulation of the 3D data is a non-trivial task due to potential vegetation, range shadows, sharp topography changes and random errors. Therefore additional editing is required to solve topology problems, improving equiangularity, reorienting inverted surface normals and smoothing. In the last stage, after optimization of the mesh for better curvature description, automatic curvature-based hole filling is used in order to deliver a smooth and continuous outcrop model.

### 3.4 Texturing

Creation of the textured 3D models requires the relationship between all the mesh vertices and the corresponding image points to be defined. This can be realised using the collinearity condition (Wolf and Dewitt, 2000) and the image interior and exterior orientation parameters.

However, because of a large overlap between the imagery, each triangle in the terrain model may be visible on several images. Due to the huge amount of redundant image data the optimal images are firstly preselected manually in order to limit the choice of the possible texture source. In the second stage of the texture optimization a decision rule to use the most suitable image as a texture source for a triangle is defined and consists of two conditions: minimum angle between the triangle normal and the image ray and the minimum distance between the camera position and the triangle (Debevec et al., 1996; El-Hakim et al., 1998; Buckley et al., 2009). Additionally, in order to eliminate disturbing effect of the small isolated patches of triangles caused by imperfect registration and radiometric differences, the texturing algorithm ensures that triangles sharing an edge are, where possible and appropriate, assigned to the same image (El-Hakim et al., 1998; Buckley et al., 2009).

### 3.5 Visualisation

For purposes of visualisation and interpretation of the virtual outcrop models, in-house software has been developed. A virtual model of an outcrop close to Green River, Utah, USA, created using the helicopter-based data, is presented in Figure 3.

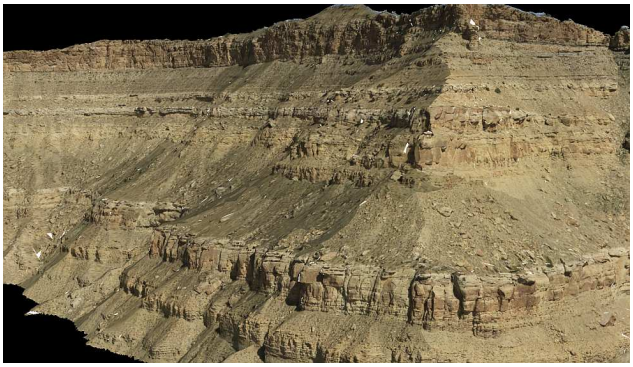

Figure 3. Virtual outcrop model of an outcrop close to Green River, Utah, USA

In order to ease visualisation of very large datasets a hierarchical set of Level of Detail (LOD) models and a spatial segmentation of the whole area are created in advance (Buckley et al., 2008b). This process is fully automated and ensures fast model visualization of large areas, as well as increasing the comfort of interpretation for the end user.

## 4. WORKFLOW IMPROVEMENTS

The quality of geological interpretation relies on the quality of the virtual outcrop models, which in turn depend on several factors: registration errors and lighting differences. Image and scanner registration errors affect the internal accuracy and coherence of the textured outcrop models. Decimation of the point cloud and mesh editing might incorporate additional distortion between the triangulated outcrop surface and the corresponding photos. An example of the visual effects of imperfect data co-registration is presented in Figure 4. Such errors lead to ambiguities during geological interpretation, which can affect the quality of the results.


Figure 4. Example of imperfect data registration

Improving coherence of the textured outcrop models is the main goal of the workflow improvements. A possibility of using the Scale Invariant Feature Transform SIFT (Lowe, 1999) operator to find corresponding points between images, and between the processed point cloud and the imagery is being investigated.

On the basis of the resulting image tie points an adjustment of the imagery orientation parameters (in a bundle) can be carried out. Especially for the models created from the helicopter based data this adjustment can bring a significant improvement of the coherence between the texture and the outcrop model. Some of the co-registration errors are due to the fact that not all of the helicopter platform vibrations and movements during the data collection are compensated for by the GNSS/INS system.

Automatic tie point extraction between the processed point cloud and the imagery aims to ease registration of the additionally taken freehand photos. This procedure is in the moment fully manual, requiring a minimum of four common points to be identified for each image, and is therefore time consuming.

The SIFT interest operator is one of the most frequently used, and is employed in computer vision in many different application fields, such as 3D matching (Delponte et al., 2006), 3D scene reconstruction (Yun et al., 2007), panorama stitching (Ostiak, 2006), robot localization (Ogawa et al., 2007) and motion tracking (Battiato et al., 2007 and Battiato et al., 2009). Application of SIFT in close-range photogrammetry is still reasonably uncommon, though it is mentioned by several authors. Kalantari documented use of SIFT for 3D modelling of

small ceramic objects (Kalantari and Kassera 2004), and Heinrichs described its application for spatio-temporal feature tracking analysis (Heinrichs et al., 2008). Investigation of the possibilities of using SIFT for co-registration of lidar intensity data and aerial images was reported by Abedini et al. (2008).
The advantage of SIFT over other interest operators traditionally used in photogrammetry, such as the Förstner operator (Forstner, 1986), Harris operator (Harris and Stephens, 1988) or Cross-Correlation, is a capability to deliver reliable results under difficult geometric and radiometric conditions (Jazayeri and Fraser, 2010; Lingua et al., 2009). This feature can potentially be very useful in attempts to locate tie points between the imagery collected from the known scanner position and the additional freehand photos. Furthermore Lingua et al. (2009) report very promising results of the SIFT performance analysis in feature extraction from terrestrial and UAV images. The authors underline the capacity of SIFT to extract and match with high accuracy huge number of homologous points on the image pairs, even with large rotations and projective distortions.

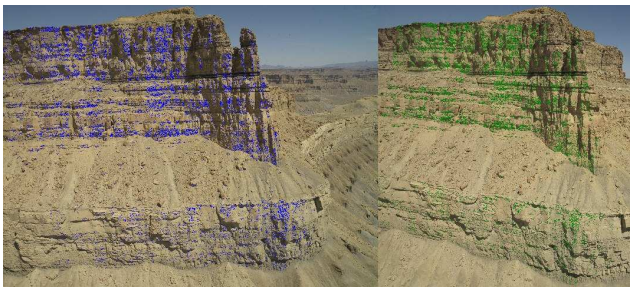

Figure 5. Homologous points extracted and matched by SIFT

The behaviour and efficiency of the SIFT interest operator has been mostly documented when applied to photos of man-made features with many edges, corners and relatively regular patterns (Picard et al., 2009). In contrast, geological outcrops have a completely different scene composition and character, with natural features, few hard edges and irregular texture. This environment can be challenging for the interest operators, especially if the distribution of the resulting points, used as tie points in later stages of processing, is of high importance. The SIFT parameters may have to be optimized (Lingua et al., 2009) in order to achieve good matching results in image areas with low texture, especially large scree slopes or areas composed of flat, homogeneous sandstone rocks.

All observations resulting from use of the SIFT operator are further combined as a free network in a bundle and adjusted. The advantage of a free network adjustment is the possibility to define the geodetic datum with minimum a priori information (Luhmann et al., 2007). This feature is of a very high importance, especially in the case of adjusting datasets acquired from the helicopter platform, where there is no possibility to collect ground control points in the vicinity of the outcrop.

Another shortcoming of the existing workflow is the fact that non-uniform lighting conditions during acquisition of images, later used for texturing of the 3D models, affect the seams between photos in the photorealistic model. An example of the unbalanced image colours/brightness is presented in Figure 6.

Figure 6. Example of varying lighting conditions

Three types of radiometric differences can be distinguished: interior image illumination variation (vignetting), global radiometric slope between images, and local illumination differences on the seam lines. Vignetting is mainly caused by the optical system and lens characteristics (Sidney, 2002). A wide range of methods of de-vignetting exists in many scientific fields, such as in microscopy, motion estimation, computer vision or astronomy, and usually the algorithms are based on analytical expressions characterizing the pattern of brightness change across the imagery (Edirlsinghe et al., 2001; Sun and Zhang, 2008, etc.). For lens models where the light fall-off effect can be sufficiently approximated using the simple cos4 relationship, this reduces the influence of vignetting significantly (Altunbasak et al., 2003; Hasler, 2004; Hanusch, 2008). More advanced correction algorithms can be found in Litvinov and Schechner (2005), Goldman and Chen (2005), Edirlsinghe et al. (2001), Lelong (2008) or Suen et al. (2006). An interesting method of local and global brightness adjustment and shadow removal is presented by Lloyd and Egbert (2002). Hanusch (2008) uses a biharmonic spline function in the brightness interpolation for local corrections. He also modifies the L (lightness) component of the images transformed to CIELAB colour space to adjust global brightness of images. The results seem to be very promising and will be further explored.

Another process worth automation in the existing data processing workflow is pre-selection of the imagery later used as a texture source. Every single photo is relevant for the final texturing stage, but significant processing time can be gained by optimization of the photo selection, especially considering the large number of redundant images and their size (uncompressed images may be 50Mb to 150Mb). Several relevant research studies are documented (Pénard et al., 2005; Allène, 2008; Baillard, 2009). All methods are based on two techniques commonly used in computer graphics for visibility analysis: the ray-tracing and z-buffering techniques (e.g. Teller and Sequin, 1991; Rogers and Earnshaw, 1987). These two techniques have now been used for decades and are very well known in the computer graphics community, so their optimization and implementation for the purposes of the outcrop model creation will be further investigated and enhanced.

## 5. CONCLUSIONS

This paper presents ongoing work to continue the advancement of the use of virtual outcrop data in geological analogue studies, with the aim of facilitating the automation of processing methodology and improving quality of the textured outcrop

models. The final aim is to increase the usability, so that spatial data becomes more accessible in earth science applications.

Application of the SIFT interest operators in combination with bundle adjustment aims not only to improve the general coherence of the textured outcrop models, but also to facilitate the integration of additionally-collected unorientated images. Automatic sorting of the imagery, together with global and local equalization of radiometric differences, will provide an optimized data source for model texturing. The final result is an improvement of accuracy and quality of the final virtual outcrops, which provides the geologist with a reliable means for digital data interpretation.

## ACKNOWLEDGEMENTS

The Research Council of Norway and the FORCE consortium are acknowledged for their support of this project (Petromaks grant 193059). Helicopter-based data collection was carried out with Helimap System AG. Thanks to Riegl Laser Measurement Systems GmbH for their continued support of the first author's institution.

## REFERENCES

Abedini, A., Hahn, M., Samadzadegan, F., 2008. An investigation into the registration of lidar intensity data and aerial images using the SIFT approach. *International Archives of Photogrammetry, Remote Sensing and Spatial Information Sciences*, vol. XXXVII (Part B1), Beijing, China, pp. 169-176.

Allène, C., Pons, J.P. and Keriven R., 2008. Seamless image-based texture atlases using multi-band blending. *Proceedings of the International Conference on Pattern Recognition ICPR 2008*. Tampa, Florida, USA

Altunbasak, Y., Mersereau, R. M., Patti A. J., 2003. A fast parametric motion estimation algorithm with illumination and lens distortion correction. *IEEE Transactions on Image Processing*, *12*(4), pp. 395-408.

Baillard, C., 2009. Automated selection of terrestrial images from sequences for the texture mapping of 3d city models. *Proceedings of the City Models, Roads and Traffic 2009 Workshop, XXXVIII*, pp. 3-4.

Battiato, S., Gallo, G., Puglisi, G., Scellato, S., 2007. SIFT features tracking for Video Stabilization. *Proceedings of the IEEE International Conference on Image Analysis and Processing*, Modena, Italy, September, 2007, pp. 825-830.

Battiato, S., Gallo, G., Puglisi, G., Scellato, S., 2009. Improved feature-points tracking for video stabilization. *Proceedings of SPIE Electronic Imaging. System Analysis for Digital Photography*, San Josè, USA, January, 2009.

Bellian, J.A., Kerans, C. and Jennette, D.C., 2005. Digital outcrop models: applications of terrestrial scanning lidar technology in stratigraphic modeling. *Journal of Sedimentary Research*, 75(2), pp. 166-176.

Buckley, S. J., Howell, J. A., Enge, H. D., Kurz, T., 2008a. Terrestrial laser scanning in geology: data acquisition, processing and accuracy considerations. *Journal of the Geological Society*, 165(3), pp. 625-638.

Buckley, S. J., Vallet, J., Braathen, A., Wheeler, W., 2008b. Oblique helicopter-based laser scanning for digital terrain modelling and visualisation of geological outcrops. *International Archives of Photogrammetry, Remote Sensing and Spatial Information Sciences*, vol. XXXVII (Part B4), Beijing, China, pp. 493-498.

Buckley, S. J., Schwarz E., Terlaky, V., Howell, J. A., Arnott, R. W. C., 2009. Terrestrial laser scanning combied with photogrammetry for digital outcrop modelling. *International Archives of the Photogrammetry, Remote Sensing and Spatial Information Sciences*, vol. XXXVIII (Part 3/W8), Paris, France, pp. 75-80.

Debevec, P.E., Taylor, C.J., Malik, J., 1996. Modeling and rendering architecture from photographs: a hybrid geometry- and image-based approach. *Proceedings of SIGGRAPH 96, New Orleans*, pp. 11-20.

Delponte, E., Isgrò, F., Odone, F., Verri, A., 2006. SVD-matching using SIFT features. *Graphical Models*, 68(5), pp. 415-431.

Edirlsinghe, A., Chapman, G. E., Louis, J. P., 2001. Radiometric Corrections for Multispectral Airborne Video Imagery. *Photogrammetric Engineering & Remote Sensing*, 67(8), pp. 915-924.

Enge, H. D., Buckley, S. J., Rotevatn, A., Howell, J. A., 2007. From outcrop to reservoir simulation model: Workflow and procedures. *Geosphere*, *3*, pp. 469-490.

Forstner, W., 1986. A feature based correspondence algorithm for image matching. *Proceedings of Symposium from Analytical to Digital*, Rovaniemi, Finland, pp. 150-166.

Goldman, D., Chen, J., 2005. Vignette and Exposure Calibration and Compensation. *Tenth IEEE International Conference on Computer Vision.* Volume 1, pp. 899-906.

Hanusch, T., 2008. A new texture mapping algorithm for photorealistic reconstruction of 3d objects. *International Archives of Photogrammetry, Remote Sensing and Spatial Information Sciences*, vol. XXXVII (Part B5), Beijing, China, pp. 699-706.

Harris, C., Stephens, M., 1988. A combined corner and edge detector. *Proceedings of 4th Alvey Vision Conference*, Alvey, UK, pp. 147-151.

Hasler, D., 2004. Mapping colour in image stitching applications. *Journal of Visual Communication and Image Representation*, 15(1), pp. 65-90.

Heinrichs, M., Hellwich, O., Rodehorst, V., 2008. Robust spatio-temporal feature tracking. *International Archives of Photogrammetry, Remote Sensing and Spatial Information Sciences*, vol. XXXVII (Part B3a), Beijing, China, pp. 51-56.

Innovmetric, 2010. Innovmetric Software Inc.: PolyWorks. Quebec, Canada. http://www.innovmetric.com/polyworks/3D-scanners/so_pointcloud.aspx?lang=en&animatesol=true (accessed 23 May 2010)

Jazayeri, I., Fraser, C. S., 2010. Interest operators for feature-based matching in close range photogrammetry. *The Photogrammetric Record*, 25(129), pp. 24-41.

Kalantari, M., Kassera, M., 2004. Implementation of a low-cost photogrammetric methodology for 3D modelling of ceramic fragments. *Proceedings of the XXI International CIPA Symposium, Athens, Greece,* October 01-06, 2004.

Lelong, C. C., 2008. Assessment of Unmanned Aerial Vehicles Imagery for Quantitative Monitoring of Wheat Crop in Small Plots. *Sensors*, 8(5), pp. 3557-3585.

Lingua, A., Marenchino, D., Nex, F., 2009. Performance analysis of the SIFT operator for automatic feature extraction and matching in photogrammetric applications. *Proceedings of the 10th CESCG Conference, 9(5),* pp. 3745-3766.

Litvinov, A., Schechner, Y. Y., 2005. Radiometric framework for image mosaicking. *JOSA A*, 22(5), pp. 839-848.

Lloyd, B., Egbert, P., 2002. Histogram painting for better photomosaics. *Computer Graphics and Imaging 2002*. Kauai, USA.

Lowe, D., 1999. Object recognition from local scale-invariant features. *Proceedings of the Seventh IEEE International Conference on Computer Vision*, volume 2, pp. 1150-1157.

Luhmann, T., Robson, S., Kyle, S., Harley, I., 2007. *Close range photogrammetry: principles, techniques and applications.* Wiley, UK, pp. 248-251.

Mountney, N.P., Howell, J.A., Flint , S.S., Jerram, D.A., 1998. Stratigraphic subdivision within the aeolian/fluvial Etjo Sandstone Formation, NW Namibia. *Journal of African Earth Sciences,* volume 27, pp. 175-192.

Ogawa, Y., Shimada, N., Shirai, Y., 2007. Environmental mapping for mobile robot by tracking SIFT feature points using trinocular vision. *Proceedings of the SICE Annual Conference, Kagawa University, Japan, 2007.*

Ostiak, P.,2006. Implementation of HDR panorama stitching algorithm. *Proceedings of the 10th CESCG Conference.* Castá-Papiernicka.

Pénard, L., Paparoditis, N. Pierrot-Deseilligny, M., 2005. 3D building facade reconstruction under mesh form from multiple wide angle views, *International Archives of Photogrammetry, Remote Sensing and Spatial Information Sciences*, vol. XXXVI (Part 5/W17), Venice, Italy, on CD-ROM.

Picard, D., Cord, M., Valle, E., 2009. Study of sift descriptors for image matching based localization in urban street view context. *Proceedings of the CMRT 2009 conference, Paris*, volume XXXVIII, Part 3/W4.

Pringle, J.K., Howell, J.A., Hodgetts, D., Westerman, A.R., Hodgson, D.M., 2006. Virtual outcrop models of petroleum analogues: a review of the current state-of-the-art. *First Break*, 24(3), pp. 33-42.

Riegl. (2010). RIEGL Laser Measurement Systems. http://www.riegl.com/ (accessed 23 May 2010)

Sidney, R., 2002. *Applied photographic optics, Third Edition*. Focal Press, pp. 254-259.

Skaloud, J., Vallet, J., Keller, K., Veyssiere, G., 2002. HELIMAP: rapid large scale mapping using handheld LiDAR/CCD/GPS/INS sensors on helicopters. *Proceedings of the Institute of Navigation GNSS Congress, Long Beach 2005.*

Suen, S. T., Lam, E. Y., Wong, K. K., 2006. Digital photograph stitching with optimized matching of gradient and curvature. *Digital Photography II. Proceedings of SPIE-IS&T Electronic Imaging*, Vol. 6069, pp. 101-112.

Sun, M. W., Zhang, J. Q., 2008. Dodging research for digital aerial images. *International Archives of Photogrammetry, Remote Sensing and Spatial Information Sciences*, vol. XXXVII (Part B4), Beijing, China, pp. 349-354.

Teller, S., Sequin, C., 1991. Visibility preprocessing for interactive walkthroughs. *Computer Graphics*, 25(4), pp. 61-69.

Vallet, J., 2007. GPS/IMU and LiDAR integration to aerial photogrammetry: Development and practical experiences with Helimap System. Voträge Dreiländertagung 27. Wissenschaftlich-Technische Jahrestagung der DGPF, pp. 19-21

Yun, S., Min, D., Sohn, K., 2007. 3D scene reconstruction system with hand-held stereo cameras. *Proceedings of 3DTV Conference*, Kos Island, Greece, May 03-07.

Wolf, P.R. and Dewitt, B.A., 2000. Elements of Photogrammetry (with Applications in GIS). Third Edition. McGraw Hill, New York, pp. 624.